

TECH LIBRARY KAFB, NM

0144565



1231 /  
8015

# NATIONAL ADVISORY COMMITTEE FOR AERONAUTICS

TECHNICAL NOTE

No. 1231

THE STREAMLINE PATTERN IN THE VICINITY OF  
AN OBLIQUE AIRFOIL

By Charles E. Watkins

Langley Memorial Aeronautical Laboratory  
Langley Field, Va.



Washington

March 1947

AFMDC  
TECHNICAL LIBRARY  
AFL 2811



## NATIONAL ADVISORY COMMITTEE FOR AERONAUTICS

## TECHNICAL NOTE NO. 1231

THE STREAMLINE PATTERN IN THE VICINITY OF  
AN OBLIQUE AIRFOIL

By Charles E. Watkins

## SUMMARY

A method for determining the streamline flow pattern of a nonviscous incompressible fluid about an oblique airfoil from the corresponding flow pattern about the airfoil in normal position is presented and illustrated with two examples. The method can be extended to account approximately for compressibility effects by applying the Prandtl-Glauert correction factor to the flow pattern that is normal to the leading edge of the airfoil. The method is expected to be useful in determining the shape of a fuselage or nacelle having a minimum of interference with the flow over a swept-back wing.

## INTRODUCTION

The problem of determining the two-dimensional flow of a nonviscous incompressible fluid about arbitrarily shaped airfoils has been solved by the application of conformal transformations (reference 1). The solution is applicable, as indicated by the term "two-dimensional," when the airfoil is considered as a cylinder of infinite length with its generating element normal to the direction of motion of the fluid. When the airfoil is oblique to the direction of motion of the fluid, the problem of determining the flow is a three-dimensional problem even with airfoils of infinite span.

Reference 2 points out that when the airfoil is oblique to the direction of motion of the fluid the streamlines must bend laterally as well as vertically in passing over the airfoil, and that the lift and flow disturbances created by an oblique airfoil of infinite span are due solely to the component of flow normal to the leading edge of the airfoil. The component of flow parallel to the axis of the airfoil has a constant value depending upon the velocity of the undisturbed fluid and upon the angle of obliquity. Calculation of the three-dimensional flow pattern

about an oblique airfoil for a given lift should therefore be possible by the superposition of a uniform velocity parallel to the axis of the airfoil on the two-dimensional flow pattern, normal to the airfoil, required to yield the given lift.

The favorable effect of sweepback (that is, reduced pressure drag) on the high-speed characteristics of a wing was shown in reference 2 to be associated with the lateral displacement of the streamlines in passing over the wing. At the root section of a swept-back wing or at the juncture of an oblique wing with a fuselage or nacelle the lateral displacement is ordinarily prevented by interference. There is, however, a possibility of shaping the fuselage or nacelle to accommodate this displacement for a given lift and thus to minimize the flow disturbance when the airfoil is at the proper attitude to produce the given lift.

The purpose of the present paper is to set up a method for calculation of the streamline pattern about an oblique airfoil and to give specific examples of the nonviscous-incompressible-fluid flow patterns about two particular airfoils. The method could be easily extended to account approximately for the effects of compressibility by applying the well-known Prandtl-Glauert correction factor to the component of flow normal to the leading edge of the airfoil.

It should be pointed out that the boundary-layer effects are expected to be more prominent in flow over an oblique airfoil than in flow over a normal airfoil. The theoretical computations, consequently, are not expected to agree as well with experiment as those for a normal airfoil.

#### SYMBOLS

$U_0$	undisturbed velocity
$U$	total local velocity
$U_0'$	component of undisturbed velocity normal to leading edge of airfoil ( $U_0 \cos \Lambda$ )
$U'$	component of total local velocity normal to leading edge of airfoil
$w$	vertical component of velocity
$\Lambda$	angle of obliquity or sweep measured from normal to direction of undisturbed flow

- $\epsilon$  angle made by resultant local-velocity vector with horizontal plane
- $\epsilon'$  angle made by vector, representing component of local velocity normal to leading edge of airfoil, with horizontal plane
- $\Omega$  acute angle between projection of resultant local-velocity vector onto horizontal plane and direction of undisturbed flow, same sign as  $\left(\frac{U'}{U_0} \cos \epsilon' - 1\right)$
- $\psi$  stream function
- $x, y, z$  Cartesian coordinates denoting any point in field of flow

#### FLOW PATTERN ABOUT AN OBLIQUE AIRFOIL

Consider an airfoil of infinite span, with camber and/or angle of attack to produce a desired lift, placed obliquely at an angle  $\Lambda$ , relative to a normal to the direction of motion of undisturbed fluid (fig. 1). At a great distance ahead of the leading edge of the airfoil the vector quantity  $U_0$  representing the velocity of the undisturbed fluid can be resolved into components normal to and parallel to the airfoil. (See fig. 2.) As indicated in the "Introduction," the component of flow  $U_0 \sin \Lambda$  parallel to the axis of the airfoil at a great distance ahead of the airfoil is the same as the corresponding component taken at any point in the field of flow; that is, the component of flow remains constant. The component normal to the wing changes with local velocity; its value  $U_0 \cos \Lambda$  at a great distance ahead of the airfoil is denoted by  $U_0'$ .

Throughout the remainder of this discussion it is clarifying to consider the flow pattern about the oblique airfoil as consisting of two separate fields of flow. The components of flow normal to the airfoil are considered as one complete flow field with undisturbed velocity  $U_0'$  and hereinafter are referred to as "normal flow pattern" or as simply "normal flow." The actual flow pattern with undisturbed velocity  $U_0$  is considered as a second, separate problem.

As previously pointed out herein and in reference 2 the lift and flow disturbances created by the airfoil are produced solely by the normal flow. The streamlines of the normal flow pattern and velocity ratio  $U'/U_0'$  along the streamlines, required to produce a given lift, can therefore be obtained from two-dimensional considerations. Reference 2 also indicates that any disturbance of the fluid created by the presence of the airfoil, whether the airfoil

is normal or oblique to the stream direction, takes place along perpendiculars to the surface of the airfoil. The vertical displacement of streamlines, therefore, is the same when considered as belonging to either the normal or actual flow field. The same reasoning applies to vertical components of velocity  $w$ .

From the foregoing considerations the direction and magnitude of the velocity at any point of a streamline belonging to the normal flow field can be compounded with the constant component of flow that is parallel to the axis of the airfoil to yield the magnitude and direction of flow at the same point in the actual flow field. (See fig. 3.) In order to obtain the lateral displacement of any streamline in the actual flow field from the corresponding streamline in the normal flow field, the vectors representing the velocities of the two fields at each point of a streamline of the normal flow field can be projected onto a horizontal plane. (See fig. 3.) This process gives a direction or slope relative to the fluid direction  $U_0$ . Since the vertical components of velocity are the same in each field, this slope can be expressed in terms of known quantities. From figure 4, it can be seen that

$$\tan (\Lambda - \Omega) = \frac{U_0' \tan \Lambda}{U' \cos \epsilon'} = \frac{\tan \Lambda - \tan \Omega}{1 + \tan \Lambda \tan \Omega}$$

and, therefore,

$$\begin{aligned} \frac{dy}{dx} &= \tan \Omega \\ &= \frac{U' \cos \epsilon' \tan \Lambda - U_0' \tan \Lambda}{U_0' \tan^2 \Lambda + U' \cos \epsilon'} \\ &= \frac{\tan \Lambda \left( \frac{U'}{U_0'} \cos \epsilon' - 1 \right)}{\frac{U'}{U_0'} \cos \epsilon' + \tan^2 \Lambda} \end{aligned} \quad (1)$$

where  $y$  is the lateral displacement of the streamlines,  $x$  is measured in the direction of undisturbed fluid  $U_0$ ,  $\Omega$  is the acute angle between the projected velocity vector of the actual flow field and the direction of undisturbed fluid  $U_0$ , and  $\epsilon'$  is the

angle that the velocity vector of the normal field makes with the horizontal plane. The lateral displacement for any value of  $x$  is then given by the evaluation of

$$y = \int_{x_1}^{x_2} \tan \Omega \, dx \quad (2)$$

provided  $x_1$  is taken far enough ahead of the airfoil for the disturbance in the flow to be negligible. The three-dimensional coordinates of streamlines in the actual flow field can now be expressed as  $x$ ,  $y$ , and  $z$  where  $z$  is the vertical displacement of streamlines common to both the normal and actual flow fields.

#### APPLICATION TO SPECIFIC AIRFOILS

In order to make clear some of the characteristics that are to be expected of flow patterns about swept-back airfoils and to outline briefly the procedure involved in deriving the pattern of flow, the method that has been discussed is applied to two generalized Joukowski or Karman-Trefftz airfoils. The generalized Joukowski or Karman-Trefftz airfoils are used because the computation of their normal flow field is relatively simple. The transformation and pertinent formulas required to obtain these airfoils and their normal flow patterns can be found in reference 3. For airfoils of more general character, the method of reference 1 may be used to obtain the normal flow pattern or it might be found expedient to obtain the normal flow pattern from wind-tunnel data.

Example 1. - A normal section of the first airfoil has a maximum thickness ratio of about 10 percent chord at 45 percent chord from the leading edge and sufficient camber to yield a lift coefficient of 0.2, relative to the normal flow, at zero angle of attack. This airfoil with some of the streamlines of the normal flow field and the velocity ratio  $U'/U_0'$  along these streamlines is shown in figure 5.

By starting ahead of the airfoil where the streamlines are almost straight and in the direction of the undisturbed flow, or where all velocity ratios are very nearly equal to unity, and by continuing behind the airfoil to where the same conditions obtain, corresponding values of  $z$  and  $U'/U_0'$  at small intervals of  $x \cos \Lambda$  can be taken from figure 5 to apply in equations (1) and (2).

The angle  $\epsilon'$  of equation (1) can be found from corresponding values of  $\Delta x \cos \Lambda$  and  $\Delta z$  by use of the equation

$$\epsilon' = \text{arc tan } \frac{\Delta z}{\Delta x \cos \Lambda} \quad (3)$$

With corresponding values of  $\epsilon'$  and  $U'/U_0'$  thus obtained, the lateral displacement  $y$  can be computed by equations (1) and (2) for any value of sweepback  $\Lambda$ .

The lateral displacements of the streamlines in the actual flow field, corresponding to the streamlines of the normal flow field shown in figure 5, are shown as functions of  $x$  in figure 6 for  $\Lambda = 45^\circ$ . It will be noted in figure 6 that no stagnation point exists in the actual field. At the point corresponding to the stagnation point of the normal flow field there is the constant component of flow parallel to the axis of the airfoil. Photographic views of a model of the airfoil fitted with an end plate that is shaped according to the vertical and lateral displacements of the streamlines are shown in figure 7. The lateral displacement of corresponding streamlines above and below the airfoil are different. (See figs. 6 and 7.) For a given airfoil at a given angle of sweepback the magnitude of this difference is related directly to the difference in local velocities on the upper and lower surfaces and consequently to the circulation.

Example 2.- A normal section of the second airfoil has a maximum thickness ratio of about 12 percent chord at about 47 percent chord from the leading edge and sufficient camber to yield a lift coefficient of 0.5, relative to the normal flow, at zero angle of attack. This airfoil with some of the streamlines of the normal flow field and velocity ratio  $U'/U_0'$  along the streamlines is shown in figure 8.

The lateral displacements of the streamlines in the actual flow field as functions of  $x$  are shown in figure 9 for  $\Lambda = 45^\circ$ . Photographic views of a model of this airfoil fitted with an end plate that is shaped according to the vertical and lateral displacements of the streamlines are shown in figure 10. The same characteristics that were pointed out for the 10-percent-thick airfoil can be noted in these figures. In figures 9 and 10 the difference in the displacements of corresponding streamlines above and below the 12-percent-thick airfoil can be seen to be much greater than the corresponding differences shown in figures 6 and 7 for the 10-percent-thick airfoil. This variation is to be expected since a much greater circulation is required for the higher lift coefficient associated with the 12-percent-thick airfoil.

DETERMINATION OF SHAPE OF BODY TO CONFORM WITH  
FLOW ABOUT OBLIQUE AIRFOIL

Since the streamlines are laterally displaced in passing over an oblique airfoil, it can be seen that if two such airfoils are brought together to form a swept-back plan form, the tendency toward a lateral bending of the streamlines on one airfoil would interfere with that on the other. Also, if an airfoil is attached obliquely to a fuselage or nacelle, these bodies would interfere with the bending of the streamlines. Such interferences might neutralize the favorable effect that would otherwise be obtained from sweepback. It is, therefore, proposed that the fuselage and nacelles can be shaped in accordance with the streamline pattern for a given design lift coefficient and, thus, minimize the interference in flow in the neighborhood of this lift coefficient.

In shaping a body to fit the streamline pattern about an oblique airfoil the difference in the displacement of streamlines above and below the airfoil must be accounted for by an offset or "shelf" in the part of the body behind the trailing edge of the airfoil. The general characteristics of the shape that bodies must have can be seen in figures 7 and 10.

Langley Memorial Aeronautical Laboratory  
National Advisory Committee for Aeronautics  
Langley Field, Va., October 2, 1946

REFERENCES

1. Theodorsen, T., and Garrick, I. E.: General Potential Theory of Arbitrary Wing Sections. NACA Rep. No. 452, 1933.
2. Jones, Robert T.: Wing Plan Forms for High-Speed Flight. NACA TN No. 1033, 1946.
3. Glauert, H.: The Elements of Aerofoil and Airscrew Theory. Cambridge Univ. Press, 1926.



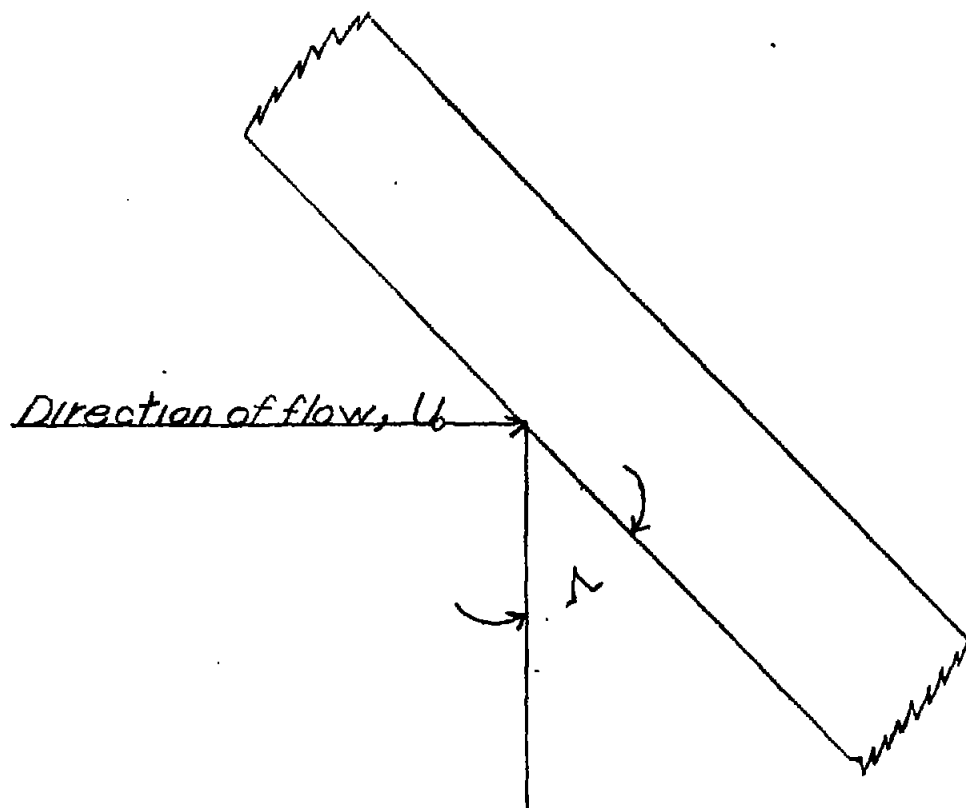


Figure 1.- Airfoil of infinite aspect ratio placed obliquely to direction of motion of undisturbed fluid or with sweep back angle  $\alpha$ .

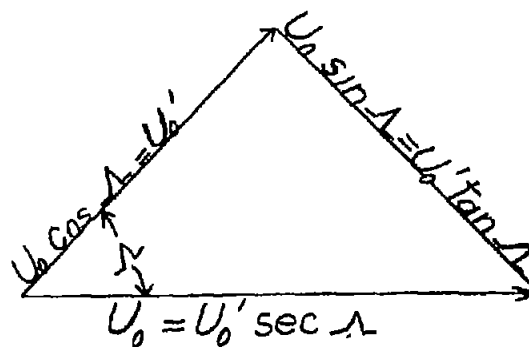


Figure 2.- Composition of velocity components at great distance ahead of airfoil.

NATIONAL ADVISORY  
COMMITTEE FOR AERONAUTICS

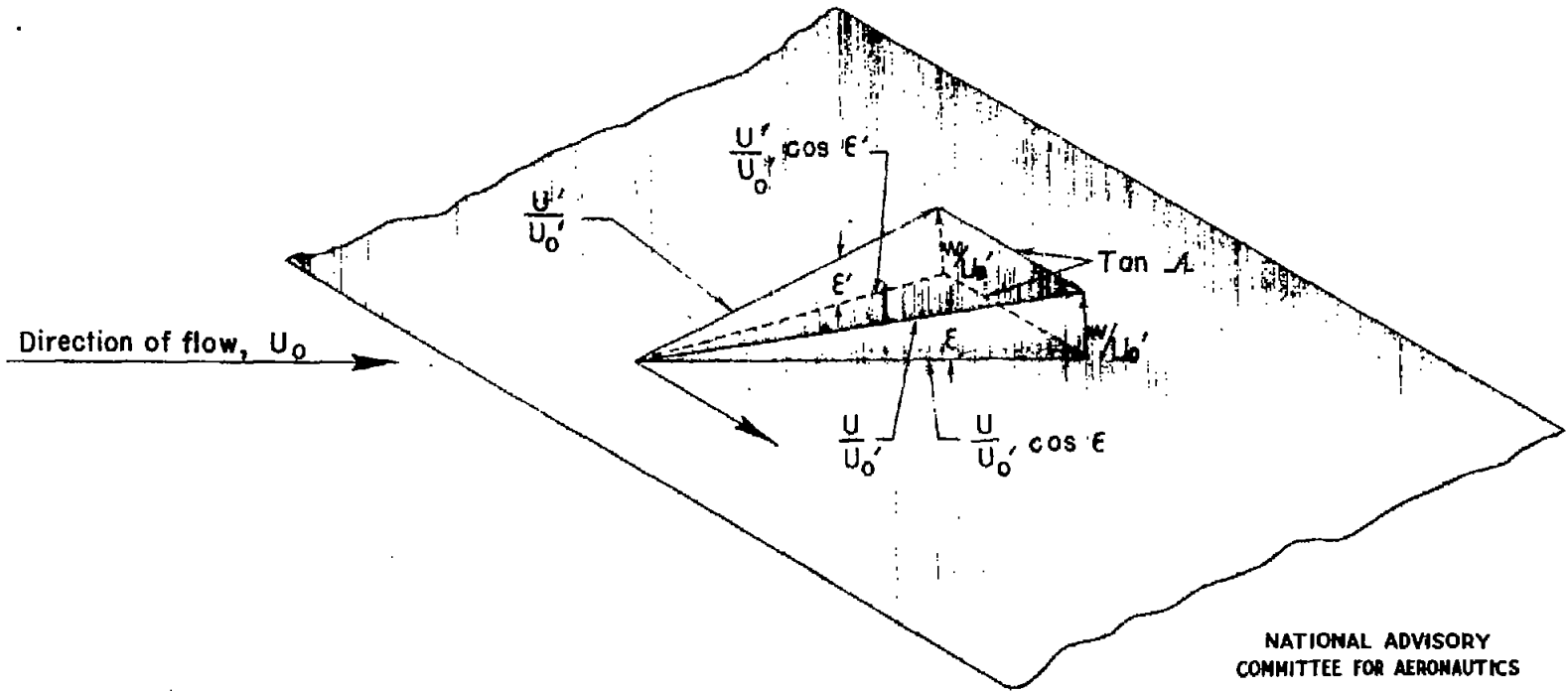
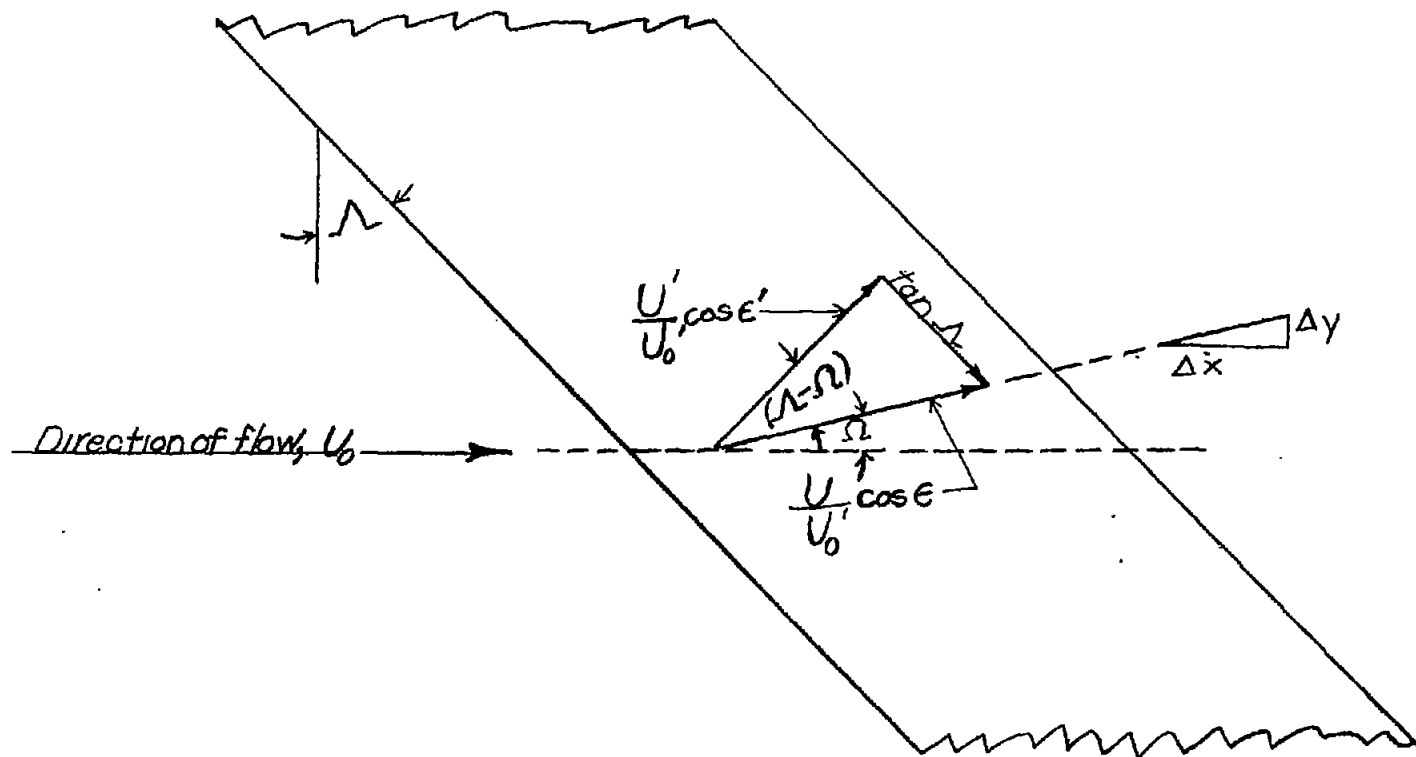
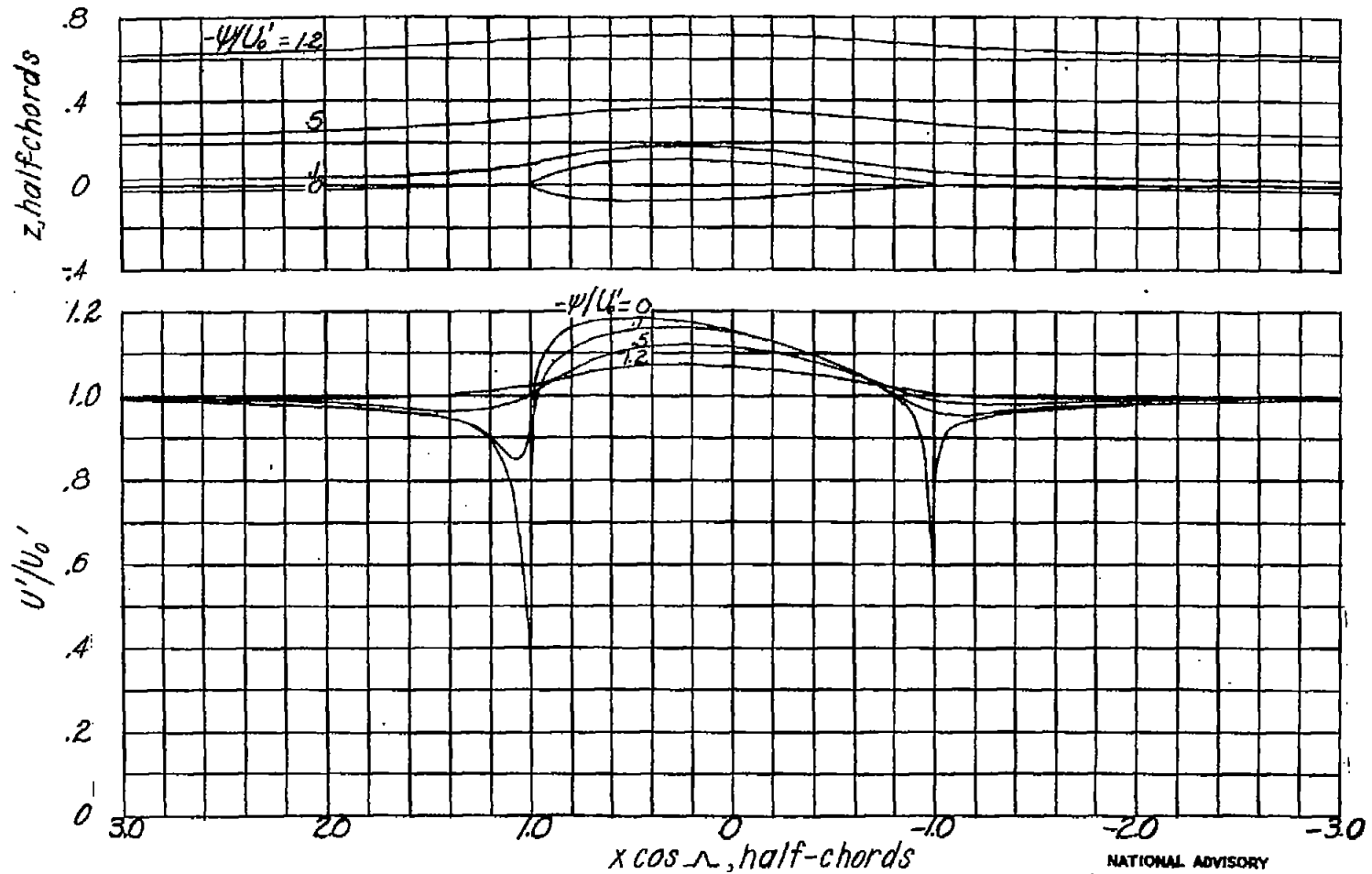


Figure 3.- Vector diagram of flow at a point near an oblique airfoil.



NATIONAL ADVISORY  
COMMITTEE FOR AERONAUTICS

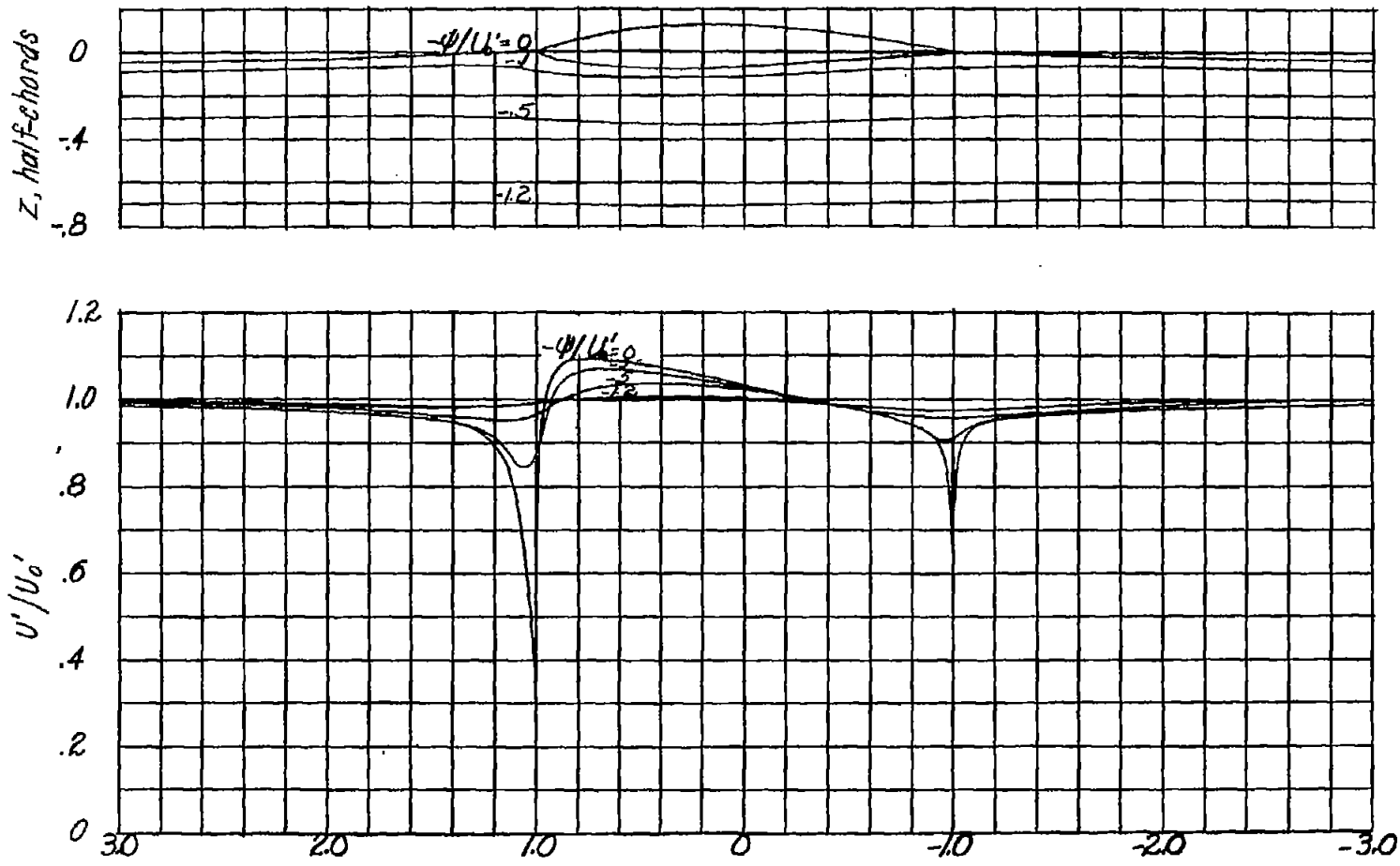
Figure 4.—Diagram of total local-velocity components projected onto a horizontal plane.



(a) Upper surface.

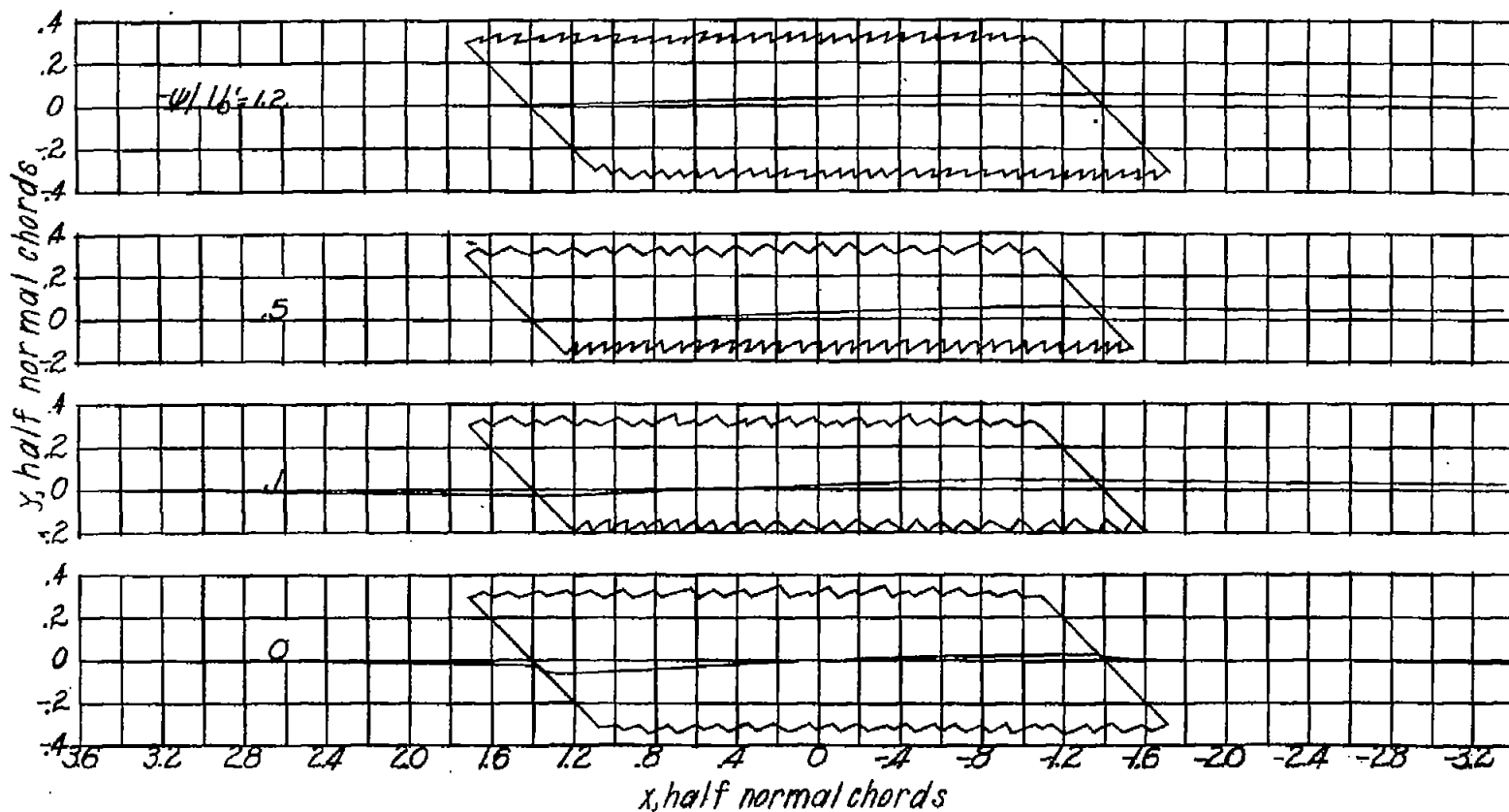
Figure 5.—Streamlines and velocity distribution for generalized Joukowski airfoil. Maximum thickness ratio, 10 percent chord; lift coefficient, 0.2; angle of attack,  $0^\circ$ .

NATIONAL ADVISORY  
COMMITTEE FOR AERONAUTICS



$x \cos \alpha$ , half-chords  
 (b) Lower surface.  
 Figure 5.- Concluded.

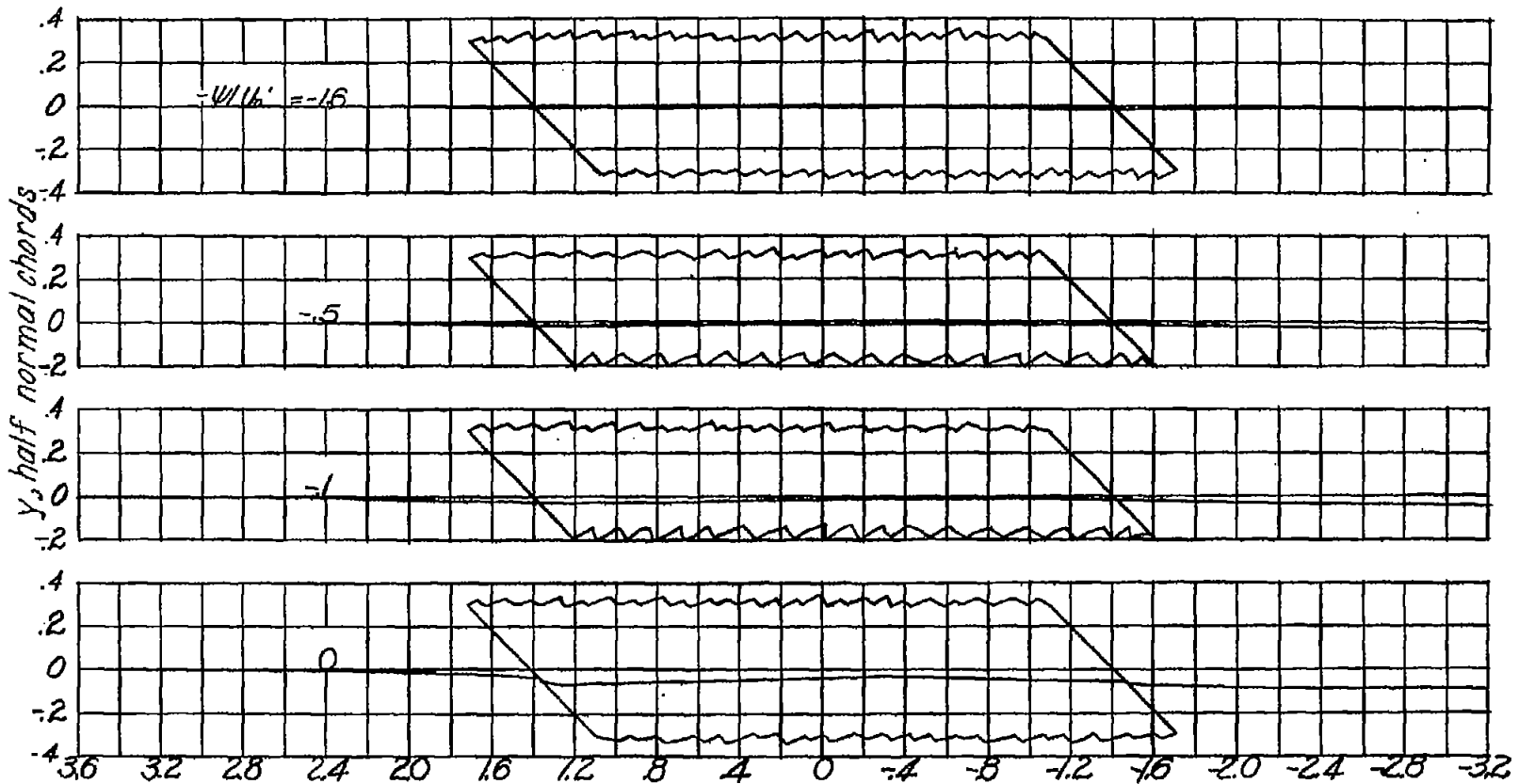
NATIONAL ADVISORY  
 COMMITTEE FOR AERONAUTICS



(a) Upper surface.

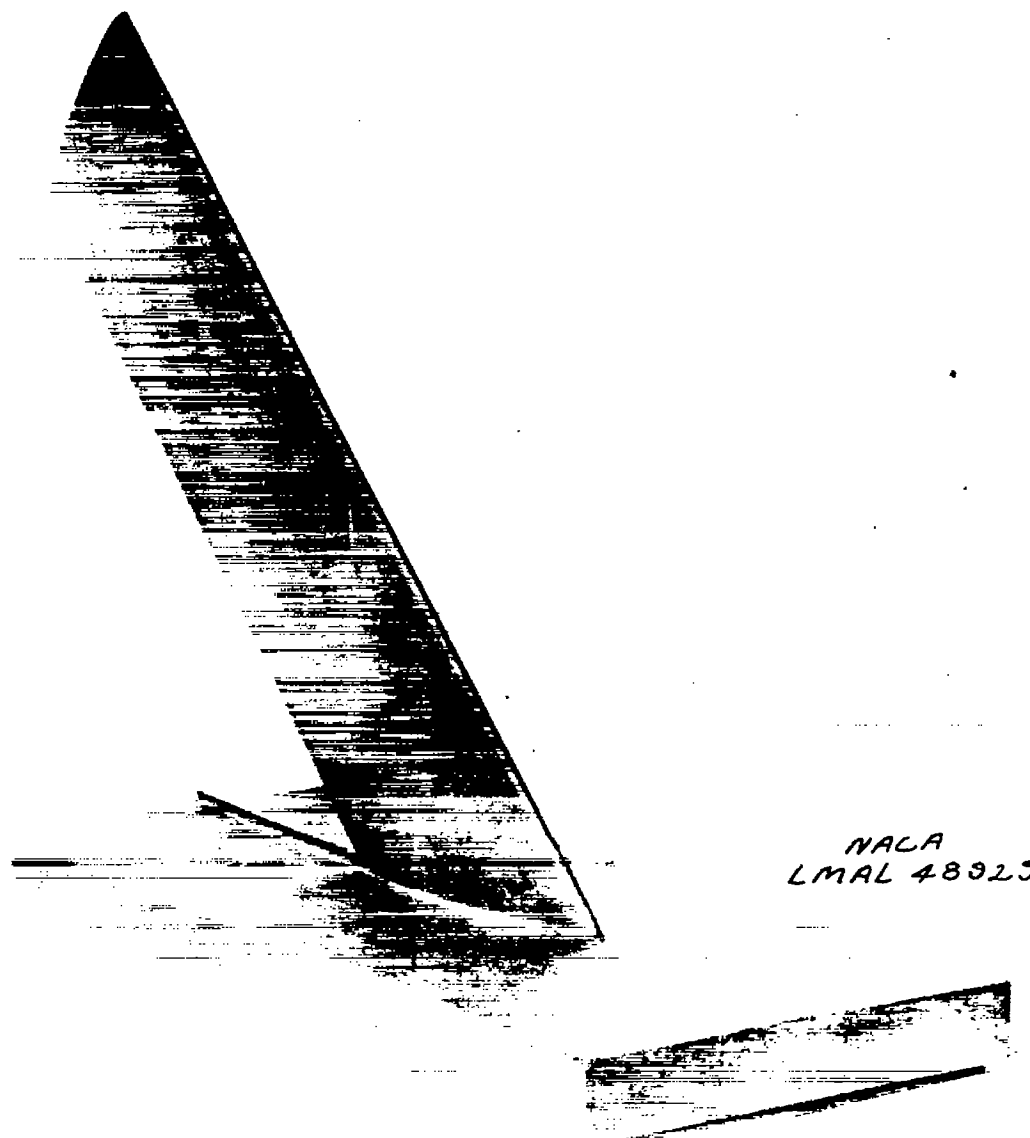
Figure 6.— Lateral displacement of streamlines about a generalized Joukowski airfoil. Maximum thickness ratio, 10 percent chord; lift coefficient relative to normal flow, 0.2; angle of attack,  $0^\circ$ ; angle of obliquity,  $45^\circ$ .

NATIONAL ADVISORY  
COMMITTEE FOR AERONAUTICS



*x, half normal chords*  
*(b) Lower surface.*  
*Figure 6.- Concluded.*

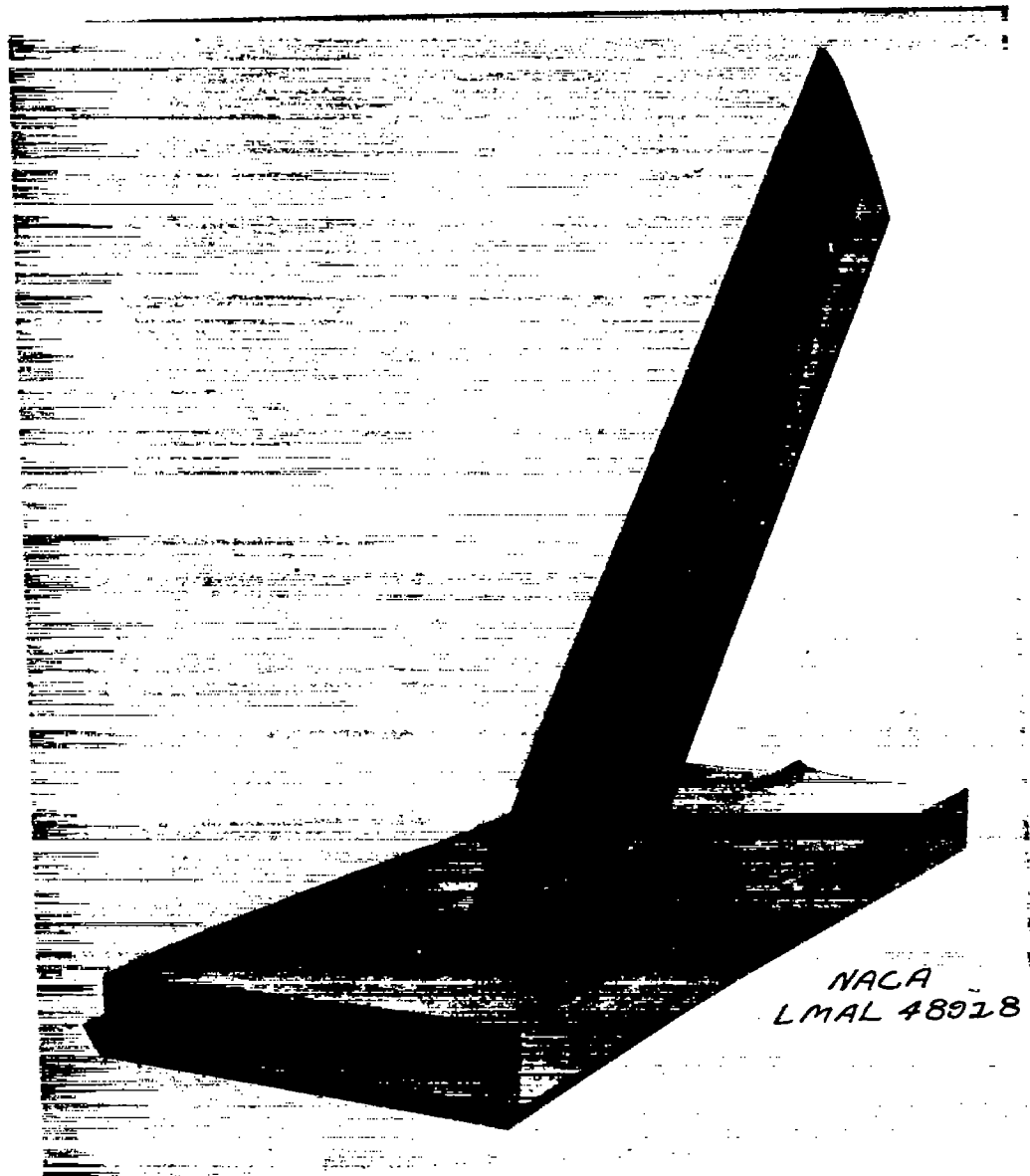
NATIONAL ADVISORY  
 COMMITTEE FOR AERONAUTICS



(a) Front view of upper surface.

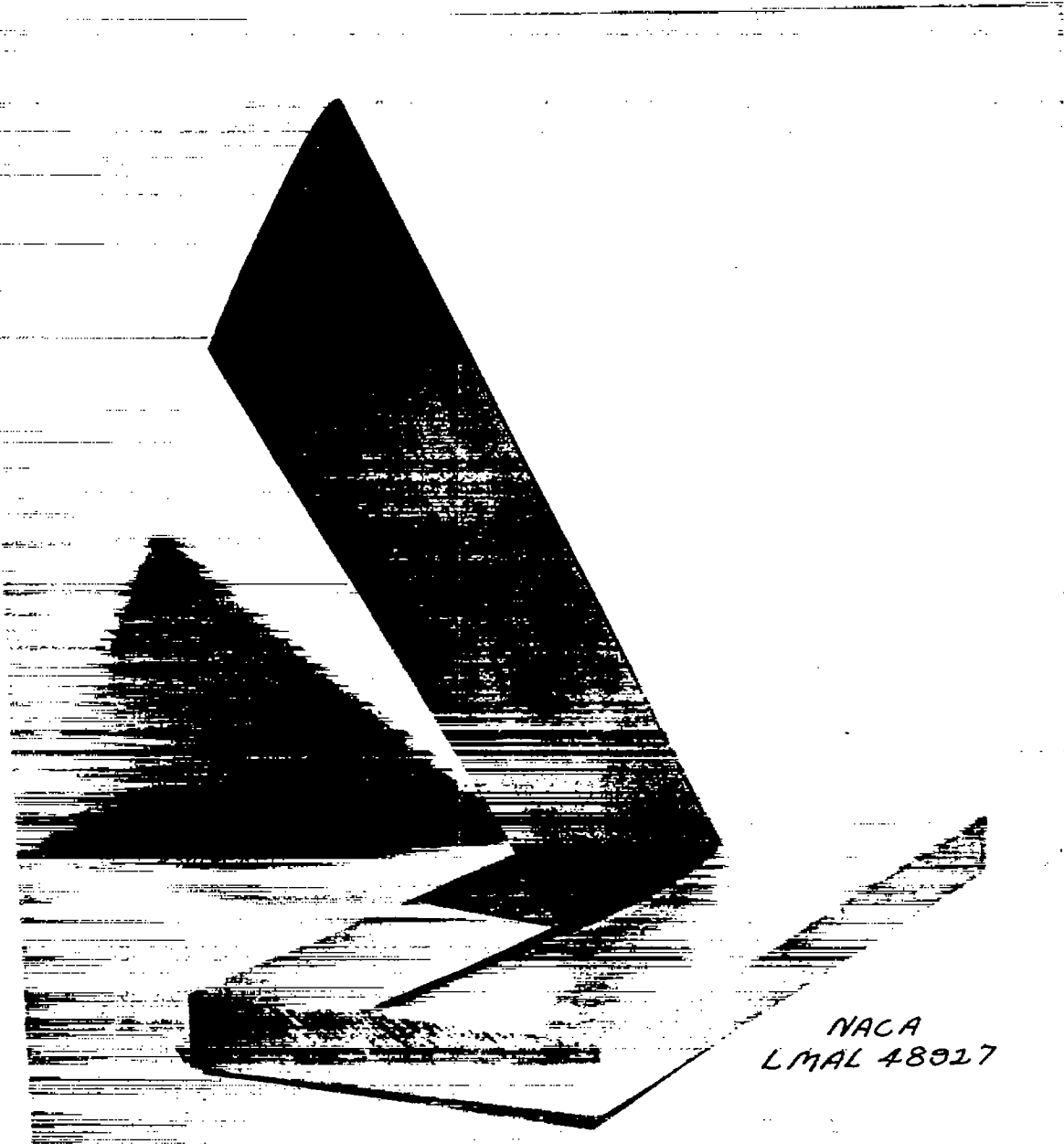
Figure 7.- Model of generalized Joukowski airfoil fitted with end plate shaped according to streamline pattern. Maximum thickness ratio, 10 percent chord; lift coefficient relative to normal flow, 0.2; angle of attack,  $0^\circ$ ; angle of obliquity,  $45^\circ$ .





(b) Front view of lower surface.

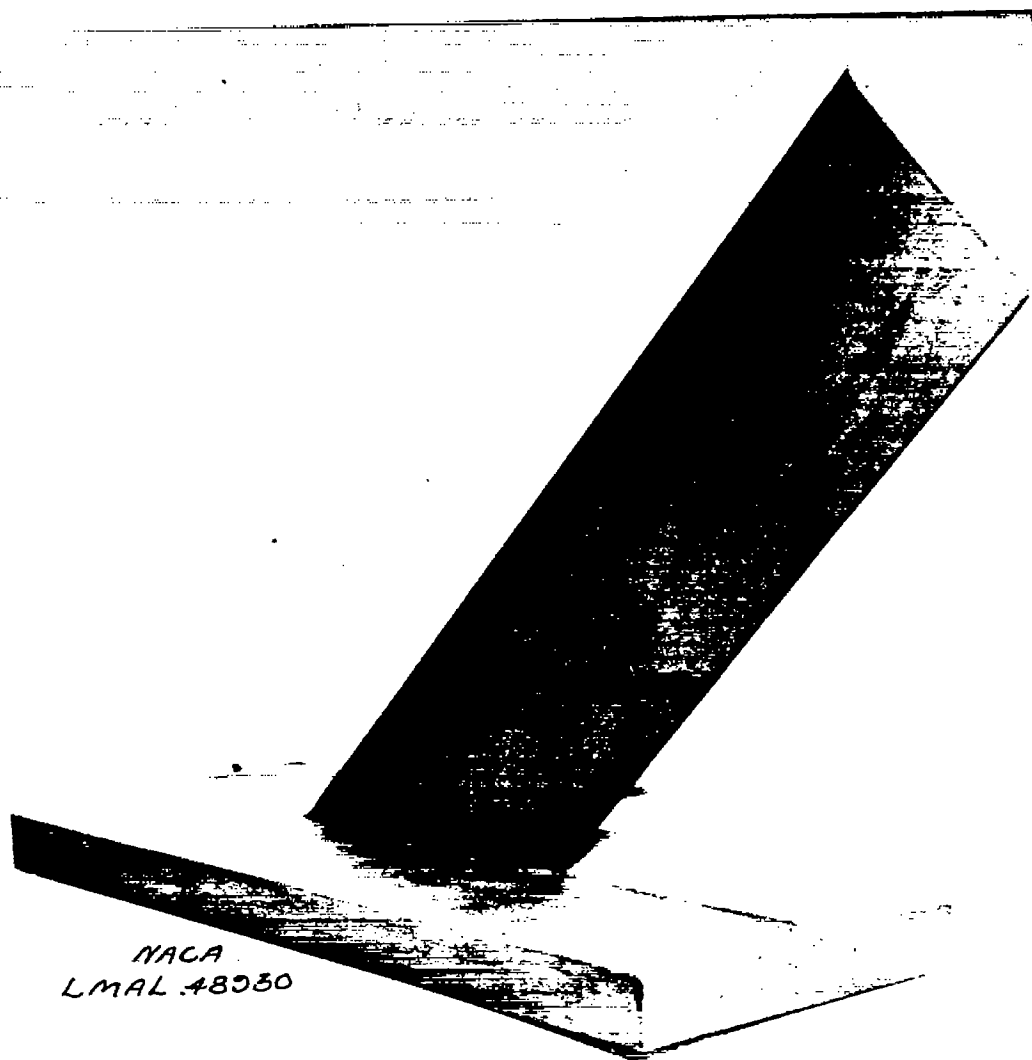
Figure 7.- Continued.



NACA  
LMAL 48917

(c) Rear view of upper surface.

Figure 7.- Continued.



(d) Rear view of lower surface.

Figure 7.- Concluded.

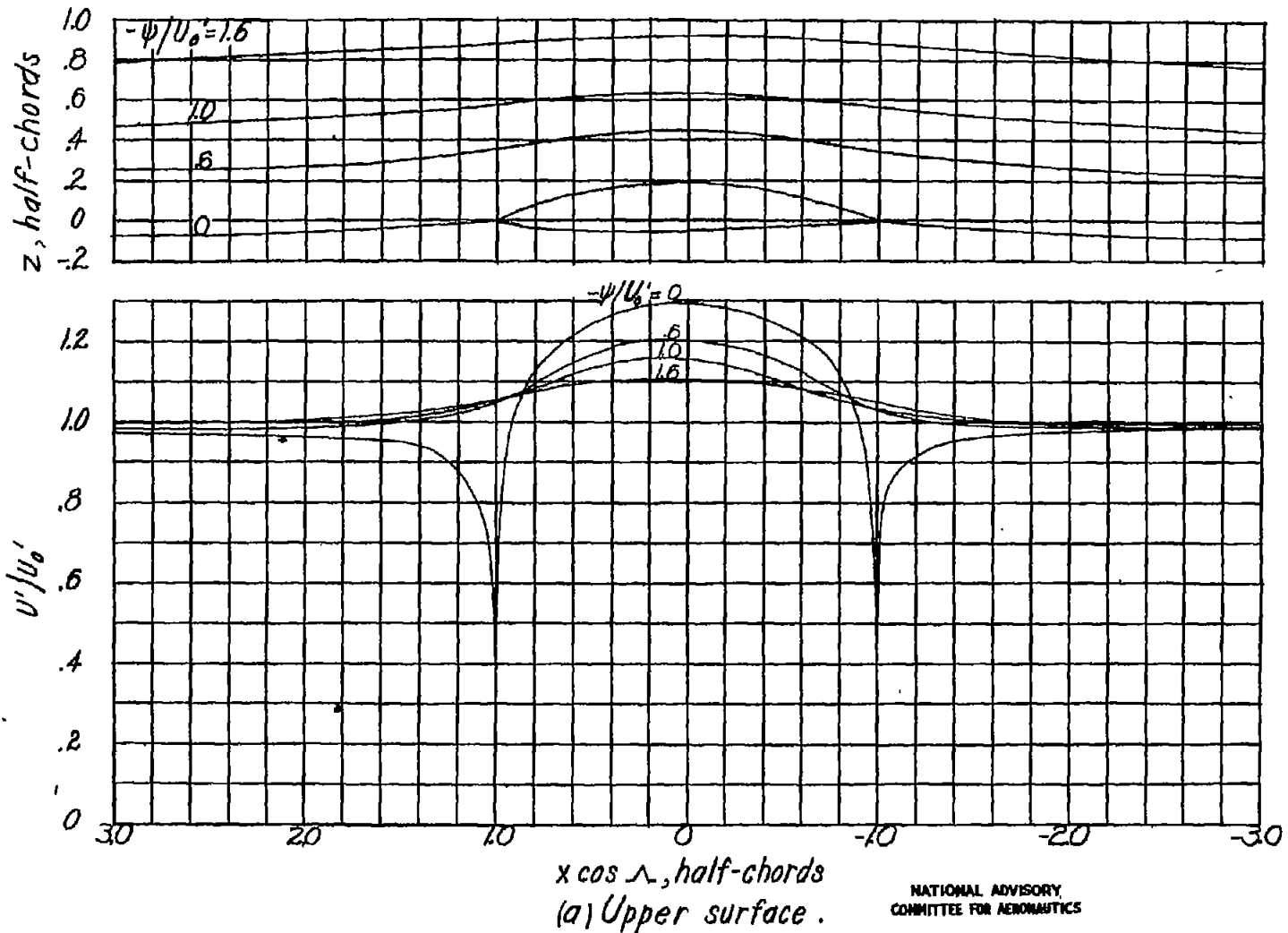
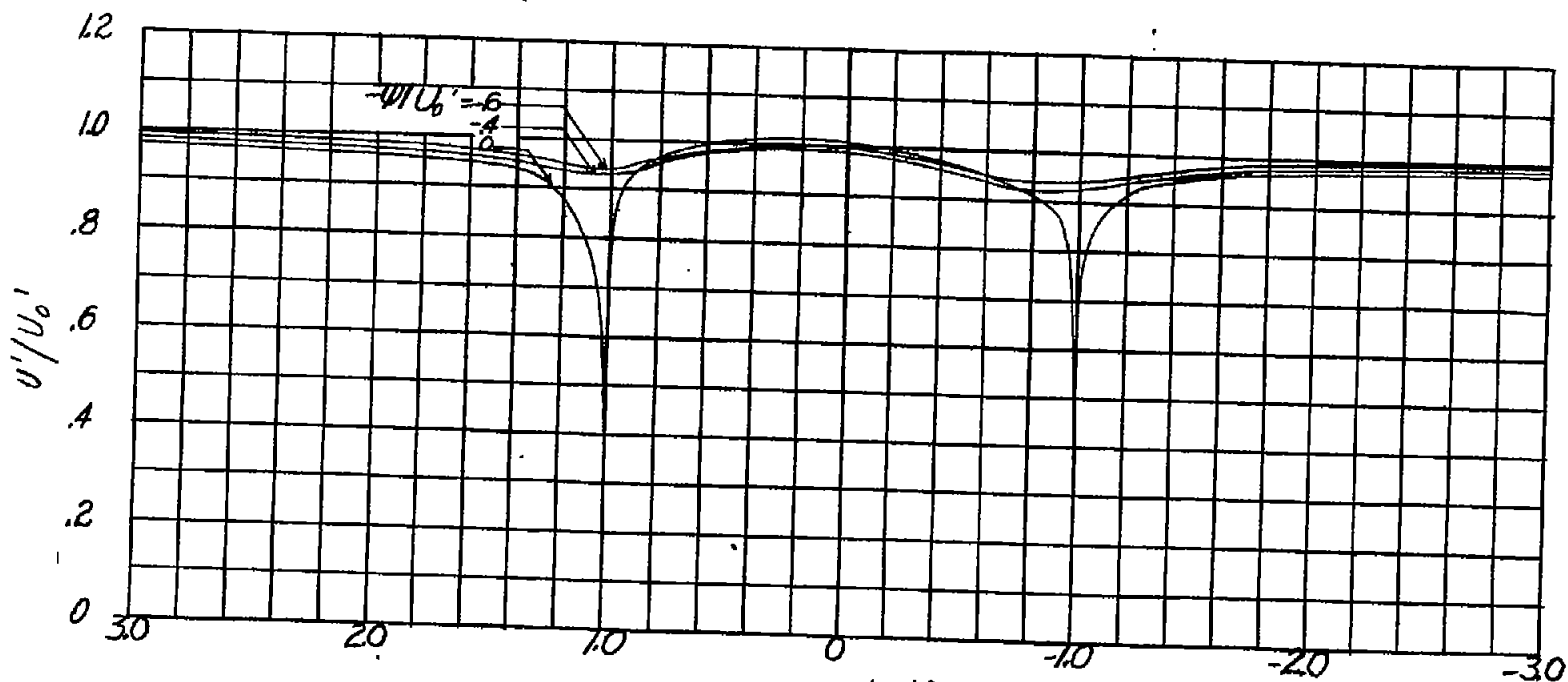
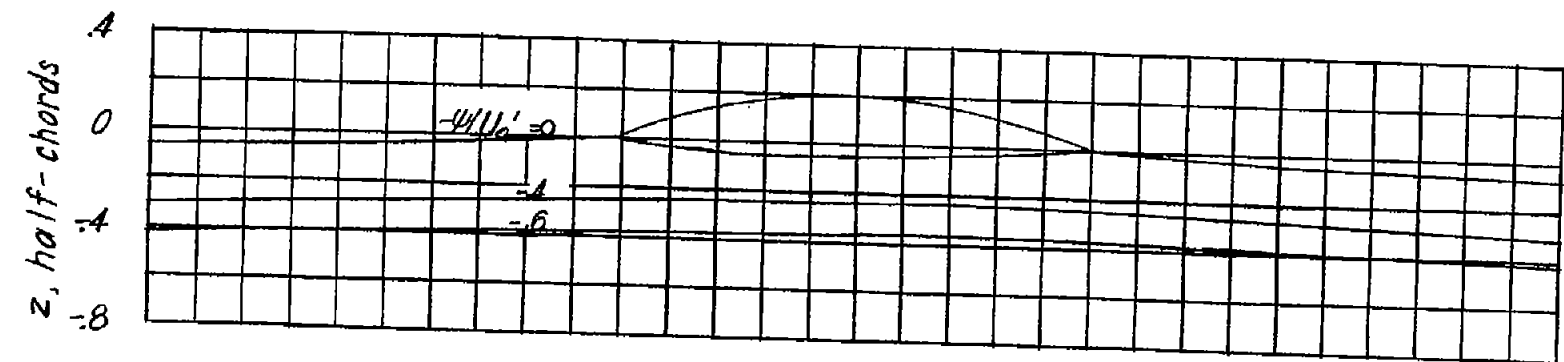


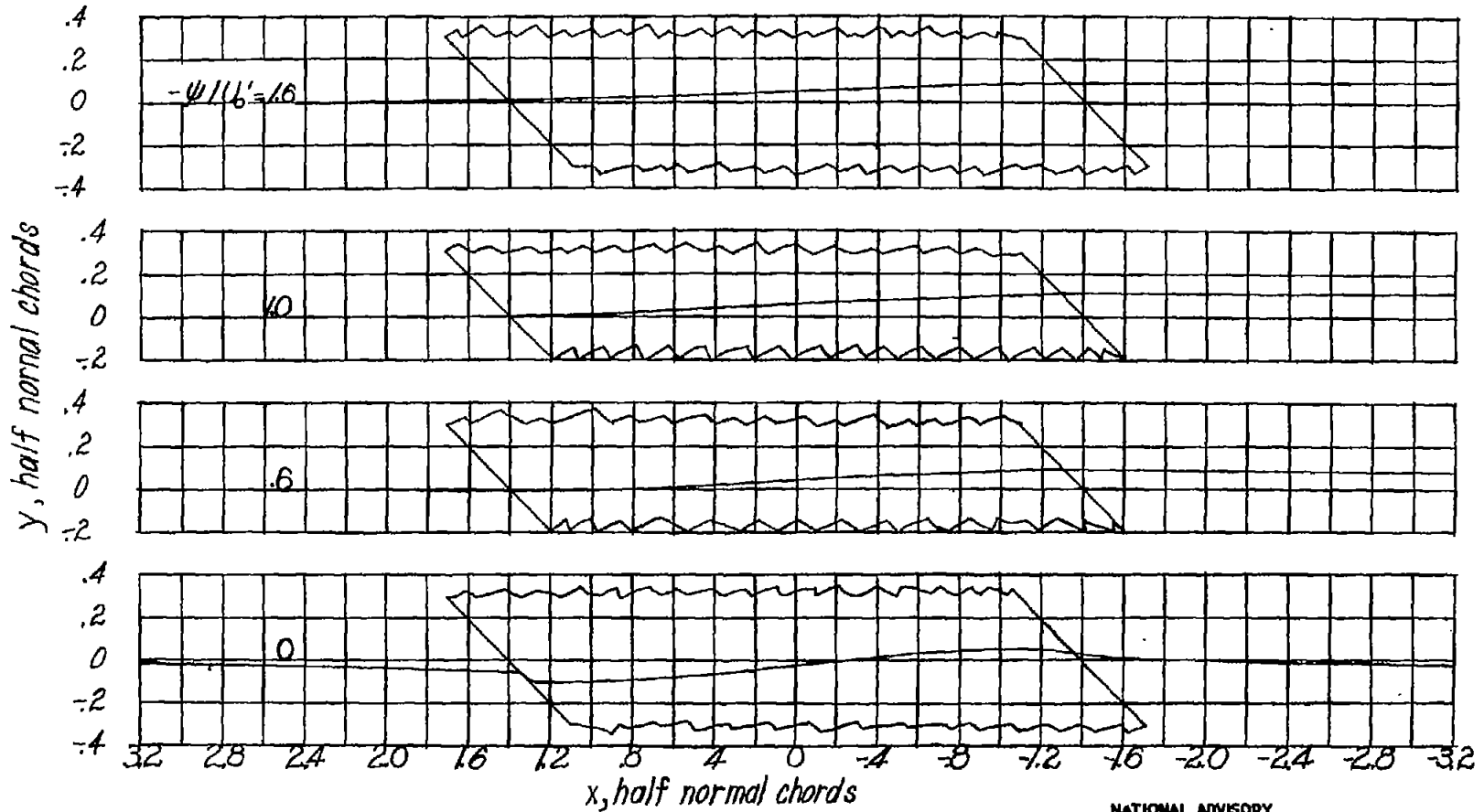
Figure 8.— Streamlines and velocity distribution for generalized Joukowski airfoil. Maximum thickness ratio, 12 percent chord; lift coefficient, 0.5; angle of attack,  $0^\circ$ .

NATIONAL ADVISORY  
COMMITTEE FOR AERONAUTICS



$x \cos \alpha$ , half-chords  
 (b) Lower surface.  
 Figure 8.- Concluded.

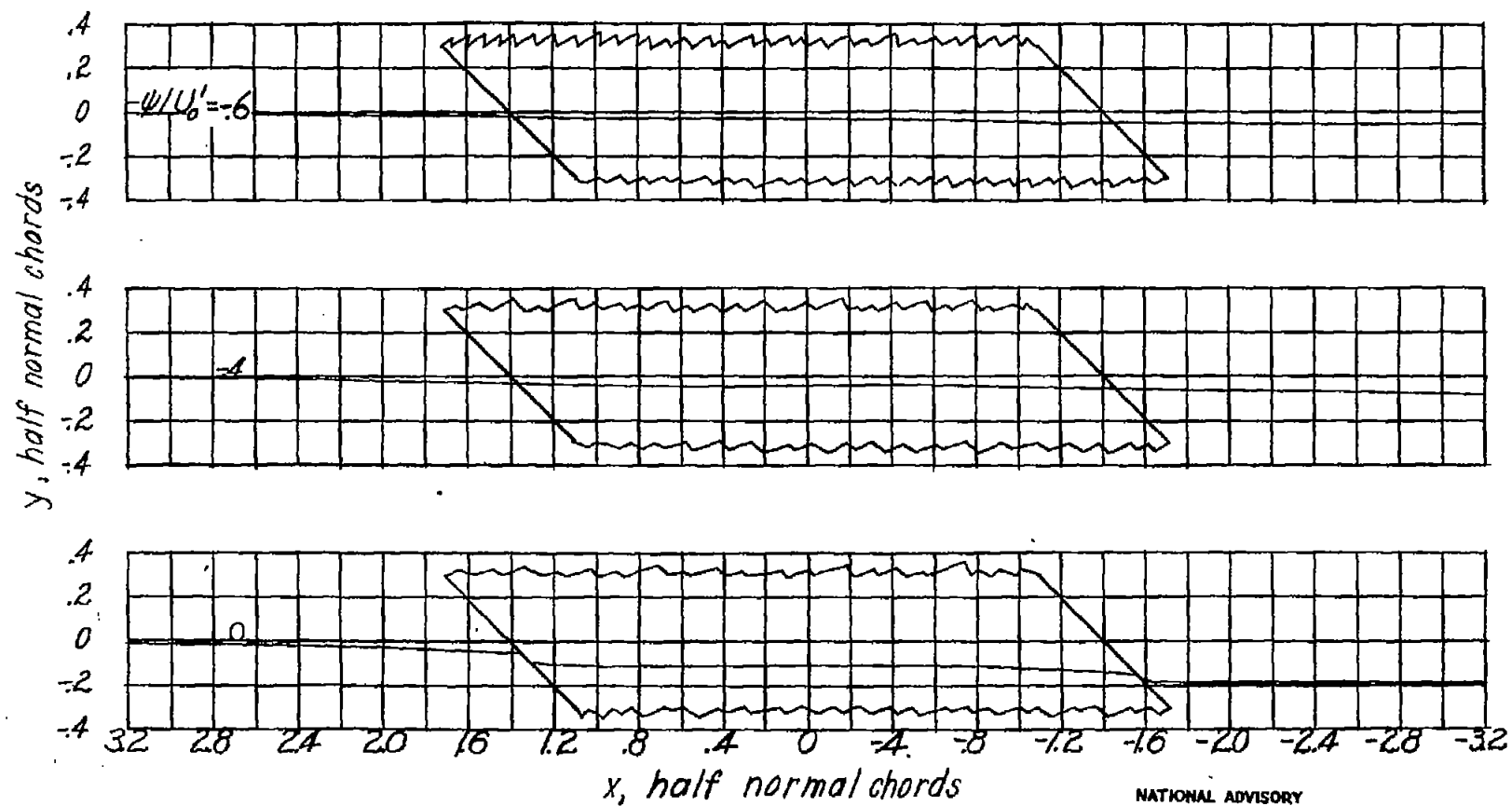
NATIONAL ADVISORY  
 COMMITTEE FOR AERONAUTICS



(a) Upper surface.

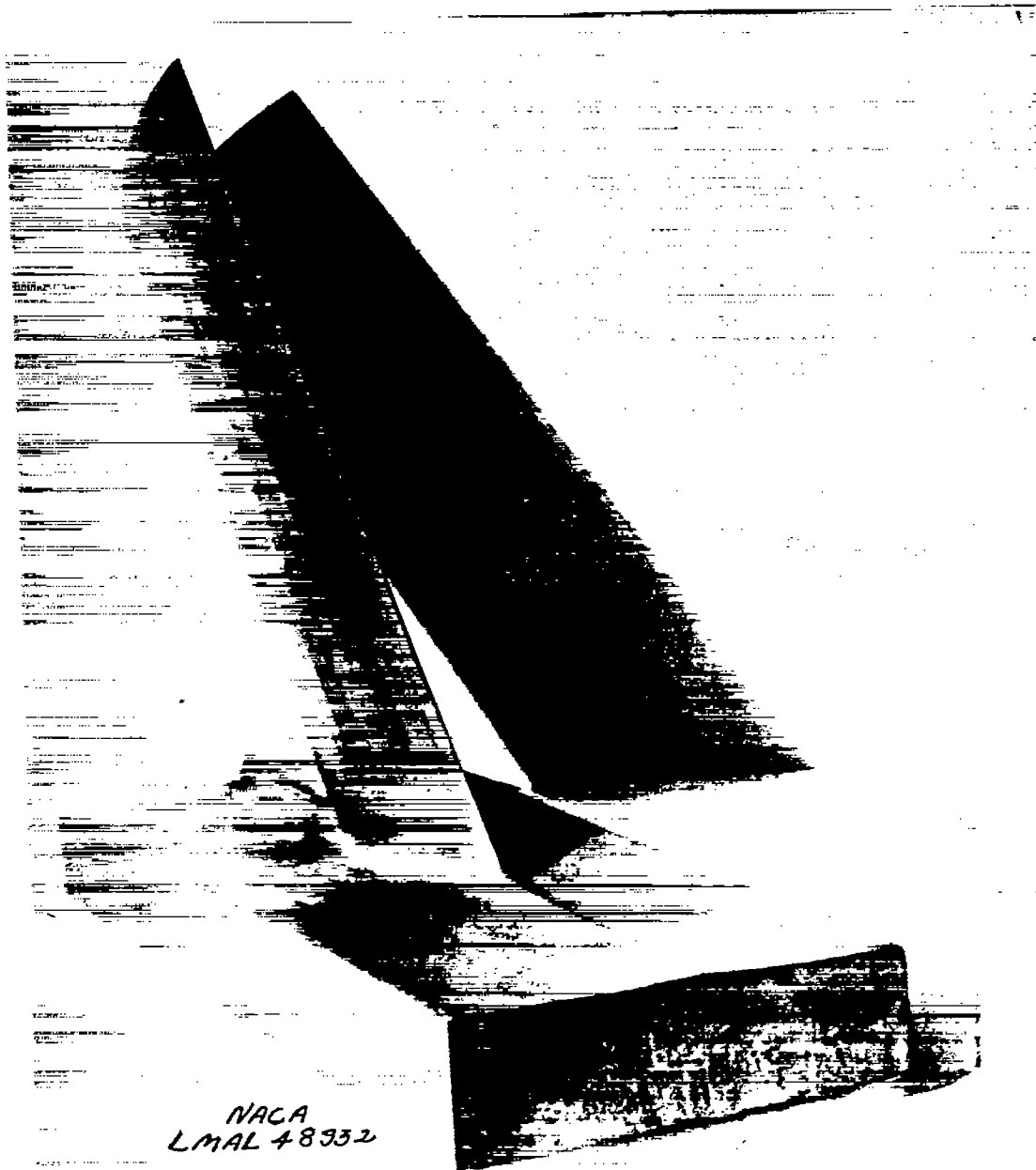
NATIONAL ADVISORY  
COMMITTEE FOR AERONAUTICS

Figure 9.—Lateral displacement of streamlines about a generalized Joukowski airfoil. Maximum thickness ratio, 12 percent chord; lift coefficient relative to normal flow, 0.5; angle of attack,  $0^\circ$ ; angle of obliquity,  $45^\circ$ .



x, half normal chords  
 (b) Lower surface.  
 Figure 9.— Concluded.

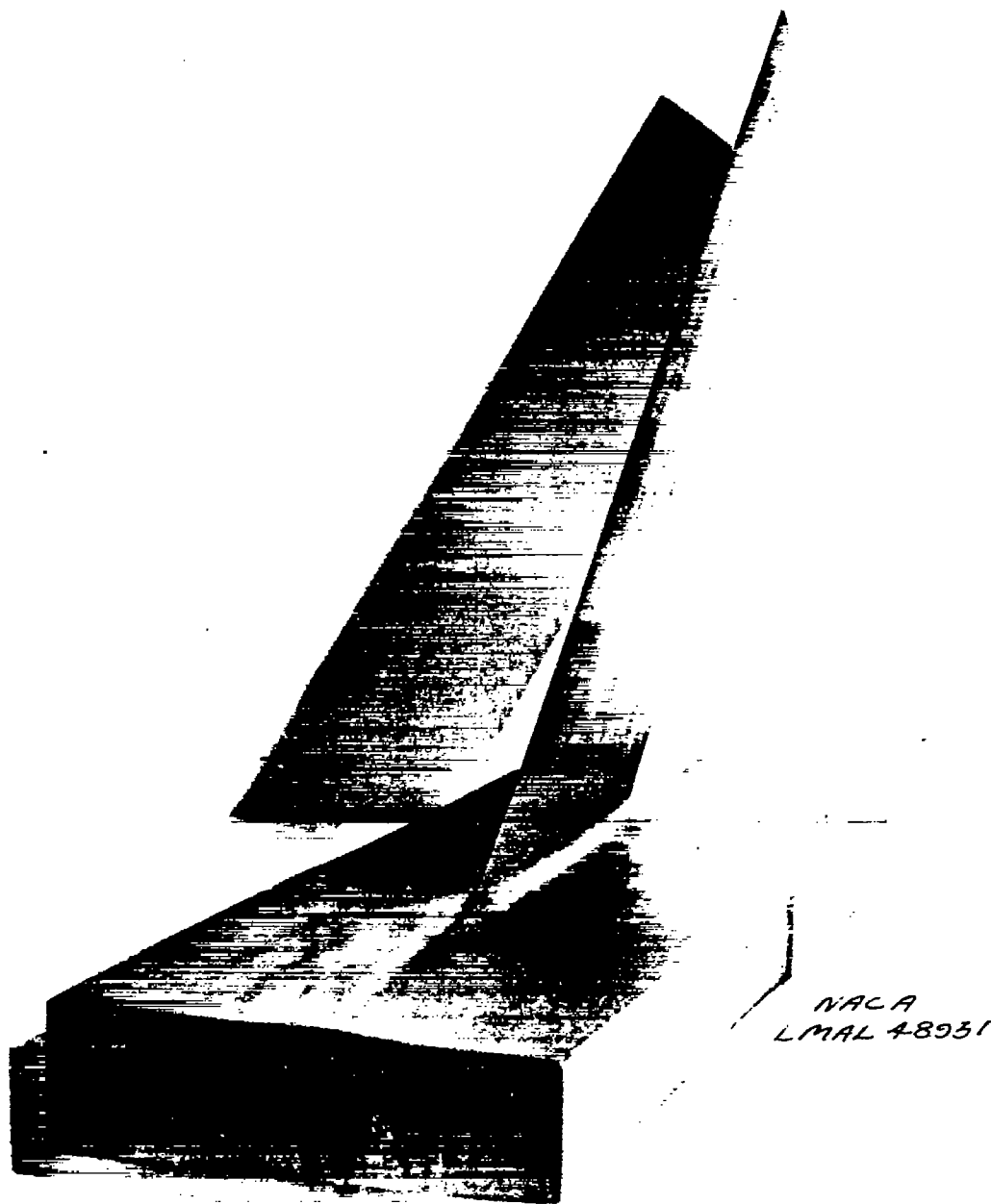
NATIONAL ADVISORY  
 COMMITTEE FOR AERONAUTICS



(a) Front view of upper surface.

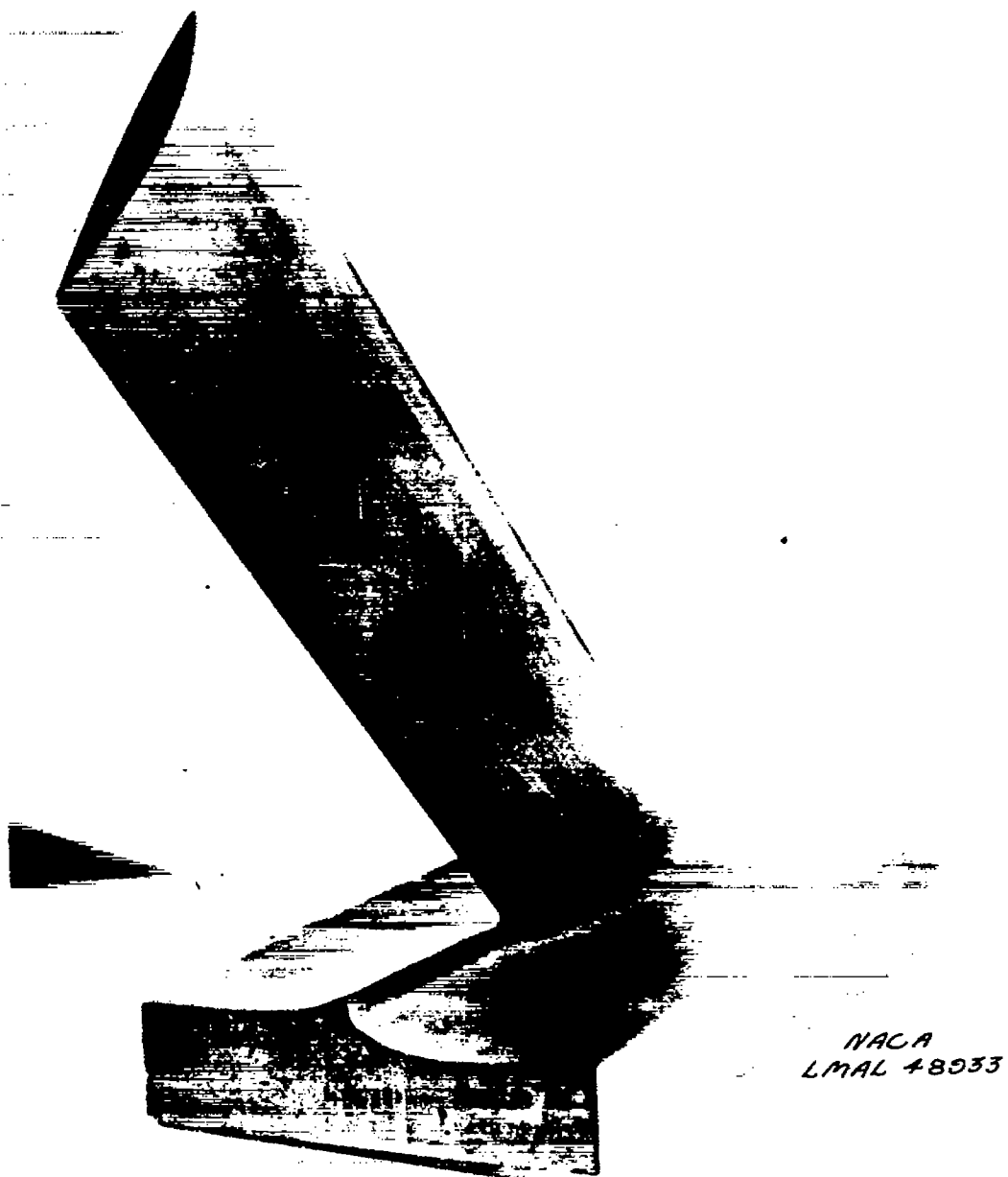
Figure 10.- Model of generalized Joukowski airfoil fitted with end plate shaped according to streamline pattern. Maximum thickness ratio, 12 percent chord; lift coefficient relative to normal flow, 0.5; angle of attack,  $0^\circ$ ; angle of obliquity,  $45^\circ$ .





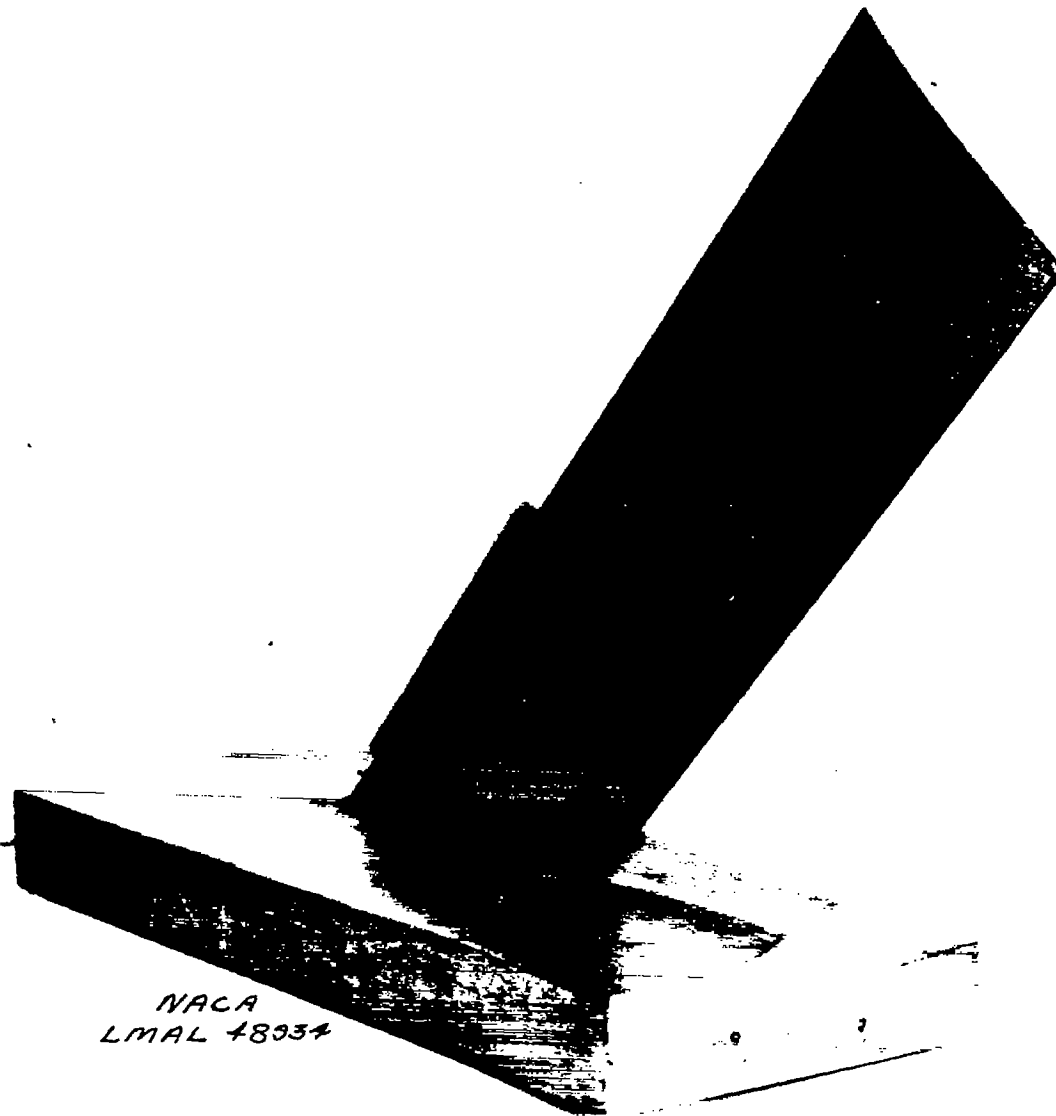
(b) Front view of lower surface.

Figure 10.- Continued.



(c) Rear view of upper surface.

Figure 10.- Continued.



(d) Rear view of lower surface.

Figure 10.- Concluded.